

Contents lists available at ScienceDirect

Science Bulletin

journal homepage: www.elsevier.com/locate/scib



Article

Megadrought and cultural exchange along the proto-silk road

Liangcheng Tan ^{a,b,c,d,*}, Guanghui Dong ^e, Zhisheng An ^{a,b,d}, R. Lawrence Edwards ^{f,g}, Haiming Li ^h, Dong Li ⁱ, Robert Spengler ^j, Yanjun Cai ^c, Hai Cheng ^{c,a}, Jianghu Lan ^{a,b}, Rustam Orozbaev ^{k,l}, Ruiliang Liu ^m, Jianhui Chen ^e, Hai Xu ⁿ, Fahu Chen ^o

- ^a State Key Laboratory of Loess and Quaternary Geology, Institute of Earth Environment, Chinese Academy of Sciences, Xi'an 710061, China
- ^b Center for Excellence in Quaternary Science and Global Change, Chinese Academy of Sciences, Xi'an 710061, China
- ^c Institute of Global Environmental Change, Xi'an Jiaotong University, Xi'an 710054, China
- d Open Studio for Oceanic-Continental Climate and Environment Changes, Pilot National Laboratory for Marine Science and Technology (Qingdao), Qingdao 266061, China
- e Key Laboratory of Western China's Environmental Systems (Ministry of Education), College of Earth and Environmental Sciences, Lanzhou University, Lanzhou 730000, China
- ^fDepartment of Earth and Environmental Sciences, University of Minnesota, Minneapolis 55455, USA
- ^g School of Geography, Nanjing Normal University, Nanjing 210097, China
- ^h Institution of Chinese Agricultural Civilization, Nanjing Agricultural University, Nanjing 210095, China
- Library of Chang'an University, Xi'an 710064, China
- ^j Max Planck Institute for the Science of Human History, Jena 07745, Germany
- ^k Research Center for Ecology and Environment of Central Asia (Bishkek), Chinese Academy of Sciences, Bishkek 720040, Kyrgyzstan
- ¹Institute of Geology, National Academy of Sciences of Kyrgyz Republic, Bishkek 720040, Kyrgyzstan
- ^m School of Archaeology, University of Oxford, Oxford OX13TG, UK
- ⁿ Institute of Surface-Earth System Science, Tianjin University, Tianjin 300072, China
- ° Key Laboratory of Alpine Ecology and Biodiversity, Institute of Tibetan Plateau Research, Chinese Academy of Sciences, Beijing 100101, China

ARTICLE INFO

Article history: Received 13 September 2020 Received in revised form 27 September 2020 Accepted 28 September 2020

Accepted 28 September 2020 Available online 20 October 2020

Keywords: Megadrought Trans-Eurasian exchange Silk Roads Arid Central Asia Mid-Holocene

ABSTRACT

Arid Central Asia (ACA), with its diverse landscapes of high mountains, oases, and deserts, hosted the central routes of the Silk Roads that linked trade centers from East Asia to the eastern Mediterranean. Ecological pockets and ecoclines in ACA are largely determined by local precipitation. However, little research has gone into the effects of hydroclimatic changes on *trans*-Eurasian cultural exchange. Here, we reconstruct precipitation changes in ACA, covering the mid-late Holocene with a U-Th dated, ~3 a resolution, multi-proxy time series of replicated stalagmites from the southeastern Fergana Valley, Kyrgyzstan. Our data reveal a 640-a megadrought between 5820 and 5180 a BP, which likely impacted cultural development in ACA and impeded the expansion of cultural traits along oasis routes. Instead, it may have diverted the earliest transcontinental exchange along the Eurasian steppe during the 5th millennium BP. With gradually increasing precipitation after the megadrought, settlement of peoples in the oases and river valleys may have facilitated the opening of the oasis routes, "prehistoric Silk Roads", of trans-Eurasian exchange. By the 4th millennium BP, this process may have reshaped cultures across the two continents, laying the foundation for the organized Silk Roads.

© 2020 Science China Press. Published by Elsevier B.V. and Science China Press. This is an open access article under the CC BY license (http://creativecommons.org/licenses/by/4.0/).

1. Introduction

Early agricultural populations in East and West Asia followed distinct trajectories of cultural development (Fig. 1a), leading to differing languages, socio-political systems, rituals, culinary traditions, cultivation practices, and domestication pathways for crops and animals [1–3]. Many scholars have noted the existence of a cultural barrier that roughly followed the mountains and deserts of ACA. Differences are visible in the types of crops and

the cultivation practices used on either side of this divide [4]. Trans-Eurasian exchange [5] led to the gradual dispersal of cultural traits across Eurasia, starting several millennia before the formation of organized and taxed commercial trade. Archeological studies indicate that wheat, barley, sheep, goats, and cattle (West Asian cultural traits) spread to East Asia during the late fifth and fourth millennium BP. Likewise, broomcorn and foxtail millet evolved under cultivation in what is now northern China and dispersed to West Asia during the fourth millennium BP [6,7] (Fig. 1c, d). Some scholars argue that the early trans-Eurasian exchange crossed the Eurasian Steppe from Europe to Asia, a model often referred to as the steppe highway [8]. However,

E-mail address: tanlch@ieecas.cn (L. Tan).

^{*} Corresponding author.

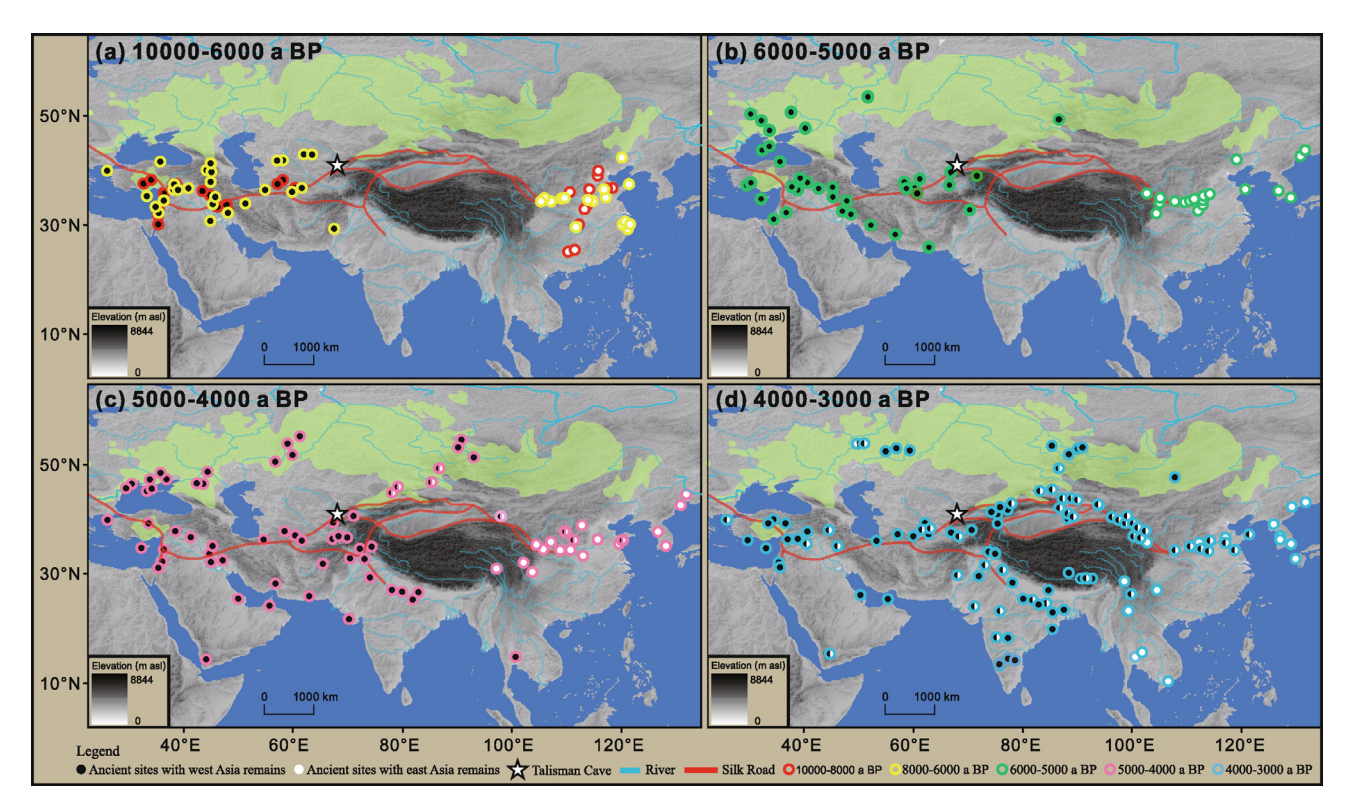


Fig. 1. Maps showing the distribution of ancient sites in ACA and the Eurasian Steppe during different millennial increments over the past 10,000 a. Representative sites in other regions of Eurasia are also shown. (a) 10,000–8000 a BP (red) and 8000–6000 a BP (yellow), (b) 6000–5000 a BP, (c) 5000–4000 a BP, and (d) 4000–3000 a BP. The black dots represent the ancient sites with West Asian cultural elements, specifically wheat, barley, sheep/goat, and cattle. The white dots represent the ancient sites with East Asian cultural elements, including foxtail and broomcorn millet. The red lines represent prominent historical routes of the Silk Roads and green shaded area represents the steppe ecoregion.

increasingly more archaeobotanical, zooarchaeological, and isotopic data suggest that the main passage for the transcontinental exchange followed the rich river valleys and alluvial slopes of the mountains to the beaded oasis passage, a continual route of communication for more than 4000 a [4,9,10] (Fig. 1b, c), designating the pre-Silk Roads (Dataset S1 online). This spatial–temporal transformation significantly influenced the development of cultures across Europe and Asia [1,2,11], yet the underlying mechanisms that drove or constrained population expansions remain unclear.

Extreme climate events, especially megadroughts lasting for decades or centuries, are thought to be a natural forcings that can contribute to the collapse of ancient imperial systems [12,13]. Shifts in surface water have been implemented in the abandonment of many major urban centers in ACA, such as those along the peripheries of the Bukhara Oasis in Uzbekistan or across the northern edge of the Kopet Dag Mountains during the third millennium BP [14]. However, whether extreme climate events in ACA played an important role in prehistoric demographic shifts and the trans-Eurasian exchange remains unexplored, due to a dearth of high-resolution climate records with accurate chronologies covering the middle to late Holocene in this region. Existing paleoclimate records reveal Holocene climate trends in eastern ACA [15–17]. These records have issues with dating uncertainty, temporal resolution, and proxy interpretation [17]. To address these uncertainties, we have produced a climate record from two stalagmites collected from Talisman Cave in Kyrgyzstan. This high-resolution (~3 a), precisely ²³⁰Th dated (dating errors are ~6‰) record allows us to correlate regional climate changes with the archaeological record, and test potential cause-effect hypotheses [18].

2. Materials and methods

2.1. Cave and stalagmites

Talisman Cave is located in the southeastern Fergana Valley in ACA (40.39°N, 72.35°E, 1486 m a.s.l), near the crossroads of the historical Silk Roads (Figs. 1 and S1 online). Mean annual precipitation in this region is ~300 mm, with more than 70% occurring during winter and spring (Figs. S2 and S3 online). The westerlies bring moisture from the Mediterranean, Black Sea, and Caspian Basin, as well as from the North Atlantic [19] (Figs. 2 and S4 online). These moisture sources also feed high-elevation snowfall and summer glacial-melt streams, which support agriculture and grassland farming in the region. Two columnar-shaped calcite stalagmites, F2 and F11, with lengths of 15.3 and 20 cm, respectively, were collected from the northern end of the cave chamber. When halved and polished, both stalagmites show clear growth layers (Fig. 3). A hiatus was determined in 114.5 mm from the top of the stalagmite F2.

2.2. Methods

Subsamples of 50–100 mg of 33 (F11) and 16 (F2) layers were drilled along the growth axis on the polished surface for U-Th dating. We followed the chemical procedure described by Edwards et al. [21] and Shen et al. [22] to separate uranium and thorium. U-Th isotopic composition and ²³⁰Th dates were determined by a multi-collector inductively coupled plasma mass spectrometer (MC-ICPMS), Thermo Fisher Neptune, at the Isotope Laboratory, Xi'an Jiaotong University [23]. Age models were established by

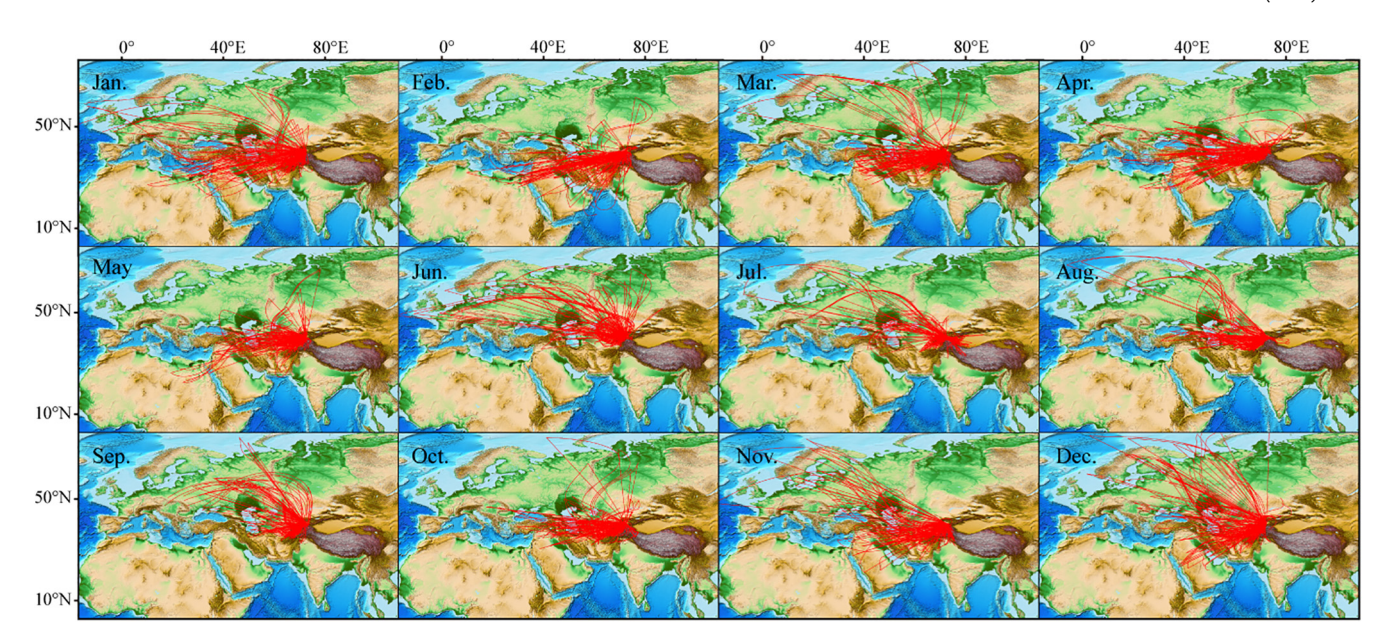


Fig. 2. HYSPLIT [20] backward trajectory analyses for moisture of Talisman Cave during different months of 2015 (data from http://ready.arl.noaa.gov/HYSPLIT.php). For each month, we computed ~120 isentropic back-trajectories (168 h) (sampled four times daily at UTC 00, 06, 12 and 18) initialized at 2000 m (above ground level).

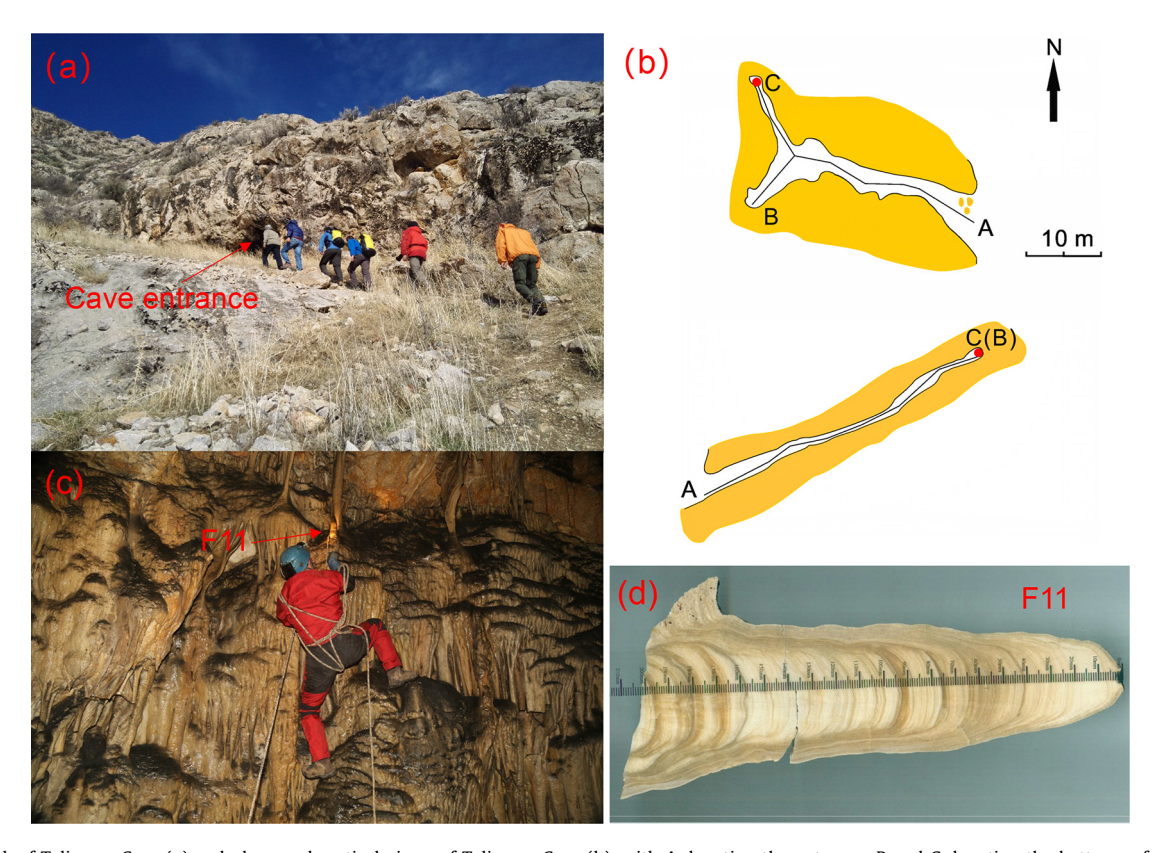


Fig. 3. Outlook of Talisman Cave (a) and plane and vertical views of Talisman Cave (b), with A denoting the entrance, B and C denoting the bottoms of two chambers, respectively. (c) and (d) are polished sections of F11 and F2, respectively. Both stalagmites were collected from a chamber at the bottom of the cave (location C in (b)).

using 5000 Monte-Carlo simulations and a polynomial interpolation procedure in the COPRA routine [24].

Stalagmite subsamples for stable isotopes (oxygen and carbon) analyses were contiguously drilled at intervals of 0.1 and 0.15 mm for F11 and F2, respectively, by using a Micromill device. Subsamples were analyzed on an IsoPrime100 gas source stable isotope ratio mass spectrometer equipped with a MultiPrep system at

the Institute of Earth Environment, Chinese Academy of Sciences (IEECAS), Xi'an, China. Reported $\delta^{18}\mathrm{O}$ and $\delta^{13}\mathrm{C}$ values were calculated with respect to the Vienna Pee Dee Belemnite (VPDB). An international standard NBS 19 was analyzed every 10–15 samples to monitor instrumentation and reproducibility. The replicates showed that the external error for $\delta^{18}\mathrm{O}$ and $\delta^{13}\mathrm{C}$ are better than 0.1‰ (2 σ), respectively.

Sr and Ca measurements were scanned along the growth axis of the ethanol-cleaned surface of F11. The measurements were carried out using the 4th generation Avaatech X-ray fluorescence (XRF) core scanner equipped with the latest variable optical XRF technology at the IEECAS [25]. The analytical settings were as follows: 30 kV and 0.03 mA with a Pd-tube, 10 s scanning time at 0.1 mm resolution, and with an irradiated area of 4 mm². Results are reported in counts per second (cps). A total of 1457 Sr and Ca measurements were scanned, respectively.

3. Results

 230 Th dating results (Table S1 online and Fig. 4) indicate that F11 continuously deposited calcite from 7774 to 656 a BP. F2 formed between 4943 and 211 a BP, with a 316-a hiatus between 3628 and 3312 a BP. This paper focuses on the prehistoric period between 7774 and 3000 a BP. F11's average dating uncertainty is \sim 6‰, and average temporal resolution of proxies is \sim 3 a, making it one of the most precisely dated and highest-resolved mid-Holocene records from ACA.

The F11 δ^{13} C and δ^{18} O values range from -8.36% to -1.16% and -14.99% to -9.73%, respectively. Significant positive correla-

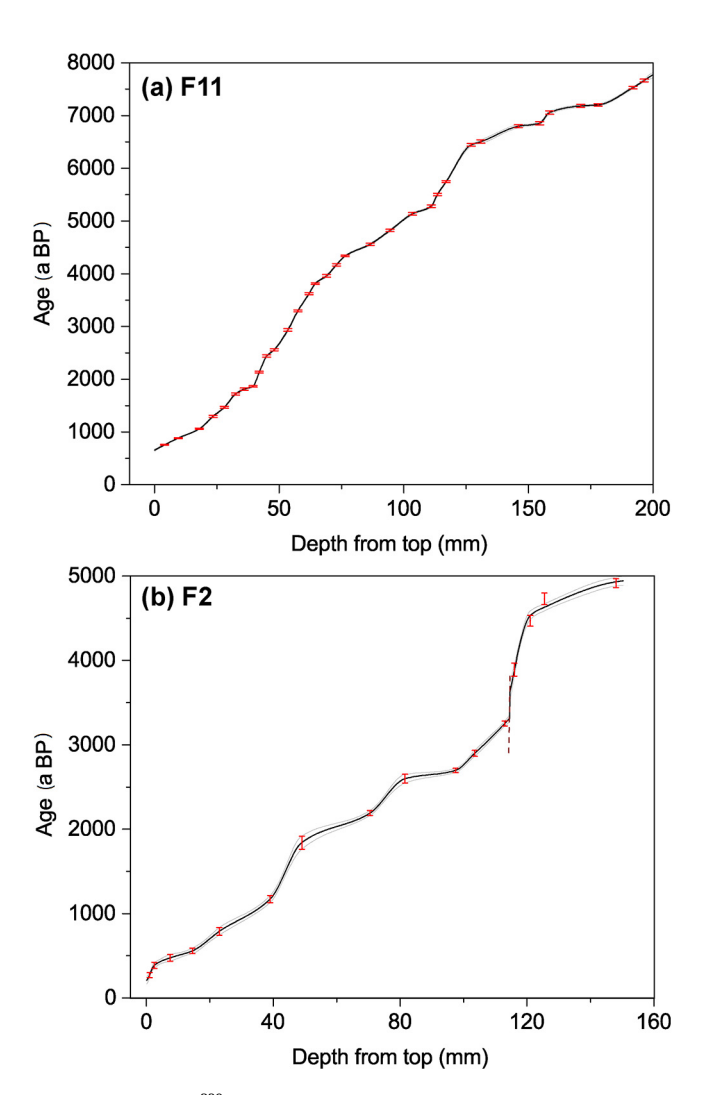


Fig. 4. (Color online) 230 Th age-depth plots of stalagmite F11 (a) and F2 (b). Age models were established using 5000 Monte-Carlo simulations [24]. Gray lines represent the 95% confidence intervals and black lines are the median ages, respectively. Error bars are 2σ error. A hiatus was determined in 114.5 mm from the top of the stalagmite F2.

tions are observed between δ^{13} C, δ^{18} O, and Sr/Ca timeseries during the period from 7774 to 3000 a BP (Dataset S2 and Table S2 online). "Hendy test" results for the F11 subsamples show no evidence of large kinetic disequilibrium effects on the δ^{18} O and δ^{13} C values of the stalagmite (Fig. S5 online). Broad similarities between the δ^{18} O profiles of F11 and F2, within the margin of dating errors, during the overlapping period are consistent with deposition at or near isotopic equilibrium (Fig. S6 online).

4. Discussion

4.1. Interpretation of proxies

Previous studies suggested vegetation type and density, soil microbial productivity, and infiltration rates could affect speleothem δ^{13} C values [26,27]. A dry climate would reduce the vegetation cover and density and soil microbial activity on one hand, and increase residence time of infiltrating water and allow more δ^{13} C-enriched bedrock to be dissolved on the other hand. Furthermore, such a lack of water enhances prior calcite precipitation in the epikarst and reduces drip rates in the cave, which in turn allows for prolonged CO₂ degassing from the drip-water. All these factors combined together, show an increasing δ^{13} C evident in the speleothem. On the contrary, a wetter climate would contribute to dense vegetation cover and microbial productivity, decreases the water-rack interaction and CO₂ degassing, resulting in more negative δ^{13} C values [26–28]. Therefore, The F11 stalagmite δ^{13} C could be viewed as reflecting local effective precipitation or precipitation-evaporation condition, with higher δ^{13} C value reflect lower precipitation-evaporation condition (mainly in winter/ spring time), and vice versa [29,30]. Prior calcite precipitation during dry conditions could also lead to higher Sr/Ca ratio in the speleothem due to preferential removal of Ca in seepage water [31]. although lower growth rates caused by insufficient seepage water during dry conditions might reduce the Sr/Ca ratio at the same

Under isotopic equilibrium fractionation conditions, stalagmite δ^{18} O changes are controlled by precipitation δ^{18} O and cave temperature [33]. Modern observations reveal lower precipitation δ^{18} O during the winter half year, but higher δ^{18} O during the summer half year (i.e., temperature effect) in the westerly controlled Eastern Mediterranean and ACA [34]. However, temperature effects cannot explain the large range of δ^{18} O values in F11 (~5‰). Winter/spring precipitation was employed to explain the stalagmite δ^{18} O variations in this region [30]. Increased winter/spring precipitation (rainfall/snowfall) brought by an enhanced Mediterranean storm track will result in lower annual mean precipitation δ^{18} O values, and cause depleted δ^{18} O values in speleothems from this region. In contrast, decreased winter/spring precipitation will enrich δ^{18} O values in a speleothem. In addition to winter/spring precipitation amount, the δ^{18} O changes in moisture sources, the so-called "source effect" could also affect the stalagmite δ^{18} O [34]. However, the significantly positive correlation between the δ^{18} O and δ^{13} C of F11 suggests precipitation as the primary controlling factor.

Significant positive correlations between δ^{13} C, δ^{18} O, and Sr/Ca suggest local precipitation exerts a common control on all. As a result, we applied principal components analysis (PCA) to the three proxy records (Table S3 online). PC1, which explains 62% of the total variance, was then used as a drought index for this region, with higher values representing less precipitation, and lower values representing more precipitation. Considering high evaporation and low precipitation in summer and autumn, we infer that our record largely reflects changes in winter/spring precipitation in

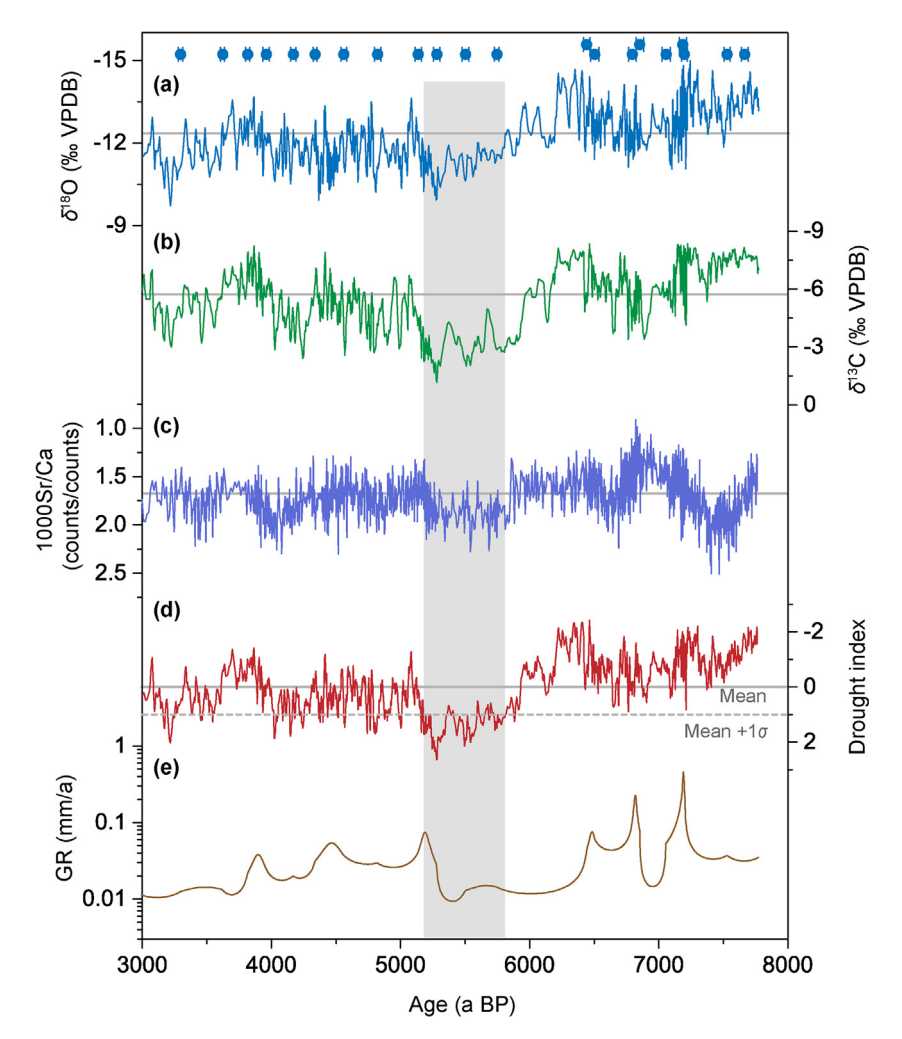


Fig. 5. Proxy records of stalagmite F11 during the mid-late Holocene. (a) δ^{18} O record; (b) δ^{13} C record; (c) Sr/Ca record; (d) drought index record represented by the PCA results of δ^{18} O, δ^{13} C and Sr/Ca records; (e) growth rate record. The grey lines in (a), (b), (c) and (d) represent the mean values of the δ^{18} O (-12.37%), δ^{13} C (-5.72%), Sr/Ca ratios (1.68×10^{-3}) and drought index (0) for the entire series, respectively. The grey bar marks the period with the drought index exceed 1σ during 5820 and 5180 a BP. Blue dots with error bars represent 230 Th dates.

this region. The index is consistent with changes in stalagmite growth rate (Fig. 5), supporting this general interpretation.

4.2. Megadrought in ACA during the mid-Holocene

Our result suggests the precipitation in ACA was relatively high before 6000 a BP, and then decreased to the lowest values at $\sim\!5280$ a BP. After that, precipitation increased with substantial centennial- to decadal-scale fluctuations, until to another dry interval between 4300 and 4000 a BP. Notably, this second period of dry conditions broadly correlates with other evidence of drought across the region [35]. Precipitation increased again starting at 4000 a BP, and rainfall was relatively high from 3930 to 3610 a BP. Precipitation then decreased, before increasing to relatively high values between 3220 and 3000 a BP (Fig. 5). The most remarkable feature of the record is the interval of abnormally positive shift between 5820 and 5180 a BP, exceeding one standard deviation (1 σ) shift relative to data from the full record (Fig. 5), indicating a prolonged period of aridity or megadrought in ACA, lasting 640 a.

A precise comparison of our records to existing Holocene stalagmite records from western ACA [29,30] is difficult because the latter are typically characterized by substantially coarser temporal resolution and less precise chronologic constraints (Fig. S7 online).

Nonetheless, some lower-resolution records (Fig. S1 online) are consistent with the megadrought idea (Fig. 6a). A 6000 a sediment sequence from Lake Son Kol in central Kyrgyzstan recorded anomalously low $\delta^{15} \mathrm{N}$ values during this period [36] (Fig. 6b). Decreased δ^{15} N indicates a reduction of input of terrestrial organic material, plausibly resulting from decreased precipitation and/or meltwater runoff during winter/spring, although summer moisture increase may have played a role [36]. During the peak of the megadrought (~5280 a BP), the level of Lake Balkhash was at least 20 m lower than at present, as indicated by abundant gypsum crystals in lake sediments [37]. In addition, multiple proxy records from Lake Issyk-Kul in northeastern Kyrgyzstan reveal a change from a fresh water open-basin to a closed-basin in the late mid-Holocene [38]. Organic δ^{13} C in loess from southern Kazakhstan reached its highest value of the entire Holocene during this period, suggesting limited moisture availability [39]. A 30000-a record of eolian deposition in the northwestern Pacific Ocean revealed the greatest dust flux ~6000 a ago, indicating severe aridity in the Asian interior [40]. The megadrought induced dust probably caused a rapid increase in coarse-grained detrital magnetite particles in the downwind region of Dali lake [41]. Although it does not cover the entire mid-Holocene, a recently published stalagmite δ^{13} C record from northern Iran [35] shows good agreement with our F11 δ^{13} C record during overlapping segments between 3770 and 4920 a BP

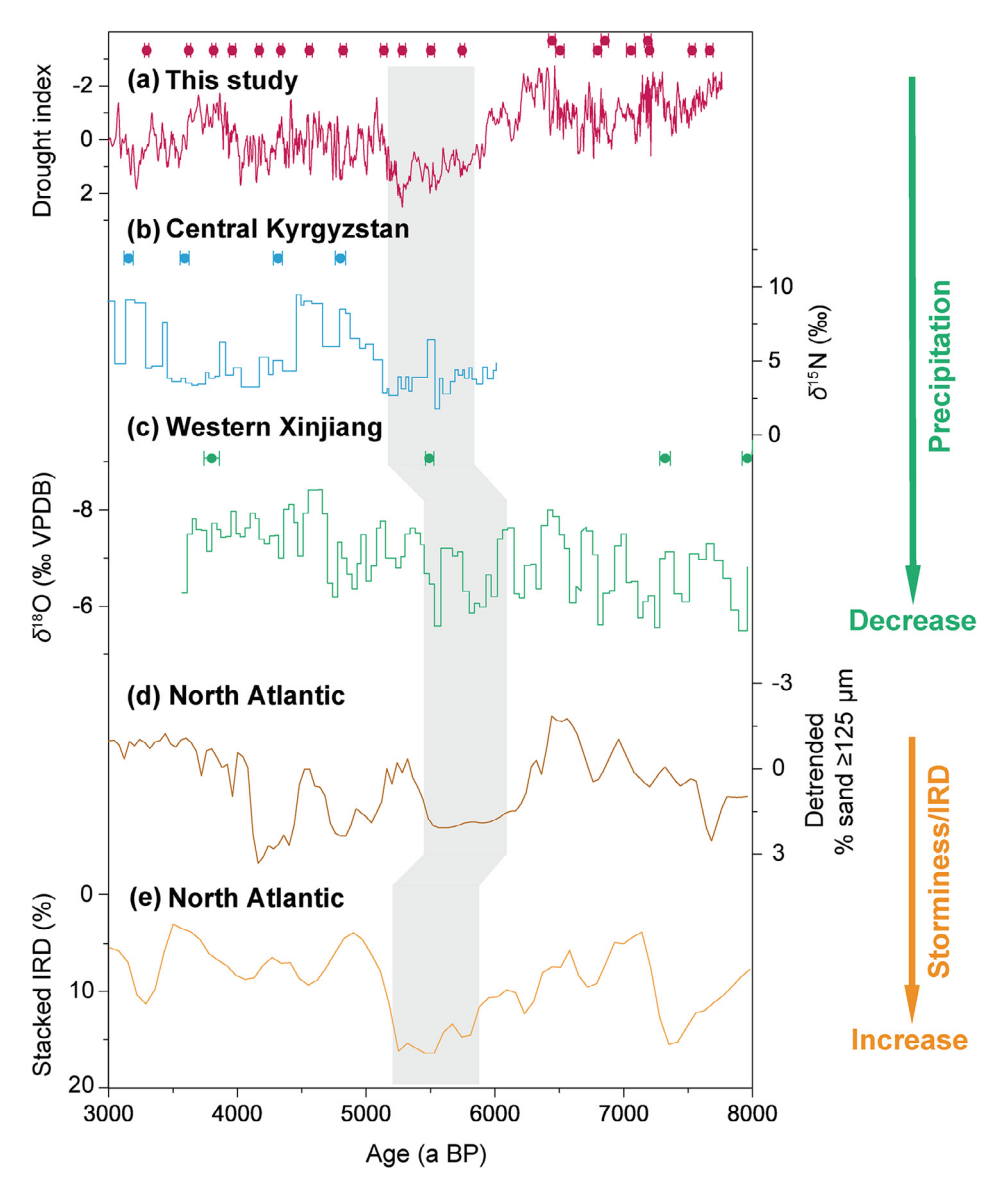


Fig. 6. Comparison of climate records in ACA, the eastern Mediterranean, and the North Atlantic. (a) Drought index record (this study); (b) δ^{15} N record from Lake Son Kol in central Kyrgyzstan [36]; (c) stalagmite δ^{13} C record from Kesang Cave in western Xinjiang, China [34]; (d) storminess activities in North Atlantic recorded by detrended coarse sand (\geq 125 μ m) percentage [47]; (e) hematite-stained grains record of Ice-Rafted Debris (IRD) in North Atlantic [50]. The grey bar marks the megadrought that occurred during 5820 and 5180 a BP. Dating points with errors of the records are also shown.

(r = 0.436, P < 0.001), implying similar precipitation variations over the western ACA.

Although long-term Holocene moisture evolution in eastern ACA, where precipitation mainly occurs in summer and autumn [42], is strongly debated [15–17,34,42,43], there is some evidence consistent with a late mid-Holocene megadrought. Substantially increased δ^{13} C in a stalagmite from Kesang Cave in the eastern Tianshan Mountains, western Xinjiang, China [29,34] is observed during this period (Fig. 6c). A megadrought might explain the slow accumulation or even cessation of peat development in the eastern Tianshan [44] at this time. A notably dry climate was also inferred for the eastern Mediterranean region, though perhaps not as severe as that in ACA. A stacked record integrating the δ^{18} O records from six lakes in the eastern Mediterranean, reveals continuously decreasing wetness during the late mid-Holocene [45]. This drying trend is supported by high δ^{13} C and δ^{18} O values in a stalagmite from Lebanon [46].

4.3. Driving force of the megadrought

A northward shift of the westerly jet may have played a role in causing the megadrought. During this period, storminess in the North Atlantic dramatically increased (Fig. 6d), indicating a northward shift of the westerly jet, akin to a present-day positive North Atlantic Oscillation(NAO) [47]. Modern observations indicate that north-shifted westerlies during a positive NAO winter correlates with reduced frequency and intensity of Mediterranean storms, decreasing precipitation in central and southern Europe, the Mediterranean and parts of southwest Asia [19]. Previous studies reveal dry climatic conditions in southern Europe [48], but wetter conditions in northwestern Europe [49] during this period, consistence with this pattern. As precipitation in ACA is mainly derived from recycled moisture from the Mediterranean, Black, and Caspian Seas [19,42] (Figs. S4 and S5 online), a weakened westerly jet and dry conditions in the Mediterranean and Caspian basin

would reduce the moisture transfer to ACA, and result in drier conditions in this region [42]. In addition, strengthened and northward shifted westerlies and storm-tracks are consistent with observations of Ice-Rafted Debris in the northwestern Atlantic during this period [47,50] (Fig. 6e). This would further decrease the sea surface temperature, and reduce the evaporated moisture transported ultimately from the North Atlantic to ACA.

4.4. Climate change and trans-Eurasian exchange

Modern observations suggest that winter/spring precipitation has an strong influence on grassland productivity in the Tianshan mountains [51]. The megadrought may have reduced productivity in mountain grasslands, at the same time reducing runoff to inland rivers, thereby affecting the oases. This may have limited prehistoric cultural development in ACA, and impeded the eastward dispersal of West Asian elements along the pre-Silk Roads (Fig. 1a. b). At the beginning of the megadrought, peoples ascribed to the Kelteminar Culture (8000-6000 a BP) migrated from oases between the Amu and Sir Rivers to the southern Siberian steppe [52,53]. In the mountain foothills of Central Asia, agropastoral populations do not migrate north or east until the fifth millennium BP. At this time, farming populations across the southern Kara Kum Desert reduced their ranges, concentrating in oases and along river valleys, such as the Murgab and Gyokser Oases and upper Amu River, as well as some locations along the northern foothills of the Kopet Dag range, where gravity fed irrigation was implemented [14,54] (Fig. 1b). While cereal cultivation is well known in parts of western ACA dating back to 6000 a BP, the eastward expansion into the desert oases, northern mountains, and eventually East Asia, did not occur until after 5000 a BP [7,55] (Fig. 1c, d). The megadrought would have hindered human movement and effectively reduced or blocked overland travel between eastern and western Central Asia along the pre-Silk Roads for these 6-plus centuries between the 6th to 5th millennia BP (Fig. 1b).

In contrast, the northward shift of the westerlies may have made conditions in the Eurasian Steppe more hospitable [19,56], enhancing pasturelands [57]. Indeed, relative light δ^{13} C values in a stalagmite record from the southern Ural Mountains during this period suggest warm/humid conditions [58]. The expansion of pastoralist populations into new grasslands that were previously sparsely populated by hunter-gatherers, may explain the archaeologically complicated phenomenon that some scholars refer to as the Yamnaya migrations during the 6th and 5th millennium BP [1-3]. Humans that utilized a similar economic strategy and may have shared similarities in material culture and genetics appear to have spread along a northern steppe/forest ecotone (Fig. 1b) when these northern steppe regions were experiencing more humid conditions [3]. Steppe-derived technologies, such as metallurgy, wheat cultivation and sheep/goat herding, started to trickle into East Asia during the 5th millennium BP (Fig. 1c) [6].

At the end of the megadrought, precipitation gradually increased in ACA, although with fluctuations (Fig. 6a). It may have resulted in greater glaciation and more prominent summer-melt streams, which could have enhanced agropastoral activities and irrigation-based farming in oases and along the alluvial fans. Starting in the fourth millennium BP, the greater investment in irrigated farming across the desert oases facilitated demographic expansions in southern ACA, what many archaeologists refer to as the Bactria–Margiana Archaeological Complex (4250–3650 a BP) [59]. Population genomics illustrate that there were greater rates of intermixing between regional populations, including the first movements of people from the steppe into southern ACA (Fig. 1c, d) [60]. Small-scale agropastoral communities developed across the foothills of ACA, and the demographic expansion resulted in cultural dispersal across ACA. This cultural boom corresponded to

the wettest period (3930–3610 a BP) in our record during the last 6000 a (Figs. 5 and S6 online). These low-investment farmers further facilitated the spread of cereal crops and herd animals into East Asia by four millennia ago. At the same time, increased precipitation [15] may have fostered the rapid rise of farming settlements in Xinjiang, China, during the early 4th millennium BP.

While further research is needed to correlate human cultural responses to shifts in climatic events, the apparent large-scale linkages are enticing. Demographic shifts, including population movement and population increase provide support for models aimed at elucidating processes affecting cultural development in ACA. After the megadrought, the mobility of agropastoral groups likely facilitated the interconnection of different oases in ACA [7,61], opening oasis routes of trans-Eurasian exchange during the 4th millennium BP (Fig. 1d), laying the foundation for the subsequent organized Silk Roads.

5. Conclusion

We reconstructed, so far, the most precisely dated and highest-resolved mid-late Holocene precipitation record for ACA, by using two replicated stalagmites from the southeastern Fergana Valley, Kyrgyzstan. Our data reveal a 640-a, previously unknown megadrought between 5820 and 5180 a BP. The megadrought likely impeded the expansion of cultural traits along the oasis routes in ACA, and diverted the earliest transcontinental exchange along the Eurasian Steppe during the 5th millennium BP. Increased precipitation after the megadrought have made conditions for the flourishing of Bactria–Margiana Archaeological Complex, facilitating the interconnection of different oases, further opened the "prehistoric Silk Roads", of trans-Eurasian exchange during the 4th millennium BP.

Conflict of interest

The authors declare that they have no conflict of interest.

Acknowledgments

This work was supported by the National Key Research and Development Program of China (2018YFA0606400), the Strategic Priority Research Program of Chinese Academy of Sciences (XDB4000000), the 2nd Tibetan Plateau Scientific Expedition and Research (2019QZKK0101), and the Youth Innovation Promotion Association of Chinese Academy of Sciences (Y201681). This work was also partly supported by the National Natural Science Foundation of China (41888101), the National Social Science Foundation of China (18ZDA172), and the National Science Foundation of United States (NSF 1702816, EAR-0908792, and EAR-1211299). It is a part of the "Belt & Road" Project of the Institute of Earth Environment, Chinese Academy of Sciences (IEECAS). We thank Dr. Sakiev Kadyrbek from the Institute of Geology, National Academy of Sciences of Kyrgyz Republic, Drs. Yougui Song, Qiang Li and Yue Li from the IEECAS, and Dr. Yaoming Li from the Research Center for Ecology and Environment of Central Asia, Chinese Academy of Sciences for their helps in the field work.

Author contributions

Liangcheng Tan directed this project. Liangcheng Tan, Guanghui Dong, Zhisheng An, and R. Lawrence Edwards formulated research questions. Liangcheng Tan, Guanghui Dong, and Fahu Chen wrote the paper. Liangcheng Tan, Hai Cheng, and R. Lawrence Edwards contributed to the ²³⁰Th dating. Liangcheng Tan, Yanjun Cai, and Dong Li performed the stable isotopic and trace elemental

analyses. Liangcheng Tan and Dong Li conducted the age model. Liangcheng Tan, Dong Li, and Rustam Orozbaev did the field work. Guanghui Dong, Haiming Li, Robert Spengler, and Ruiliang Liu analyzed the archeological sites. All authors discussed the results, edited, and commented on the manuscript.

Appendix A. Supplementary materials

Supplementary materials to this article can be found online at https://doi.org/10.1016/j.scib.2020.10.011.

References

- [1] Allentoft ME, Sikora M, Sjögren KG, et al. Population genomics of Bronze Age Eurasia. Nature 2015;522:167–72.
- [2] Damgaard PDB, Marchi N, Rasmussen S, et al. 137 ancient human genomes from across the Eurasian steppes. Nature 2018;557:369–74.
- [3] Zhou X, Yu J, Spengler RN, et al. 5200-year-old cereal grains from the eastern Altai Mountains redate the trans-Eurasian crop exchange. Nat Plants 2020;6:78–87.
- [4] Spengler R. Fruit from the sands: the Silk Road origins of the foods we eat. Berkeley: University of California Press; 2019.
- [5] Sherratt A. In: Contact and exchange in the ancient world. Honolulu: Hawaii University Press; 2006. p. 30–61.
- [6] Long T, Leipe C, Jin G, et al. The early history of wheat in China from ¹⁴C dating and Bayesian chronological modelling. Nat Plants 2018;4:272–9.
- [7] Spengler RN, Frachetti MD, Doumani P, et al. Early agriculture and crop transmission among Bronze Age mobile pastoralists of Central Eurasia. Proc R Soc B-Biol Sci 2014;281:20133382.
- [8] Christian D. Silk Roads or Steppe Roads? The Silk Roads in world history. J World Hist 2000;11:1–26.
- [9] Frachetti M. Multi-regional emergence of mobile pastoralism and non-uniform institutional complexity across Eurasia. Curr Anthropol 2012;53:2–38.
- [10] Kuzmina EE. The prehistory of the Silk Road: encounters with Asia, Philadelphia: University of Pennsylvania Press; 2008.
- [11] Haak W, Lazaridis I, Patterson N, et al. Massive migration from the steppe was a source for Indo-European languages in Europe. Nature 2015;522:207–11.
- [12] Weiss H. Megadrought and collapse. Oxford: Oxford University Press; 2017.
- [13] Sinha A, Kathayat G, Weiss H, et al. Role of climate in the rise and fall of the Neo-Assyrian Empire. Sci Adv 2019;5:eaax6656.
- [14] Kasparov AK. Environmental conditions and farming strategy of the protohistoric inhabitants of south-central Asia. Paléorient 1994;20:143–9.
- [15] Chen F, Jia J, Chen J, et al. A persistent Holocene wetting trend in arid central Asia, with wettest conditions in the late Holocene, revealed by multi-proxy analyses of loess-paleosol sequences in Xinjiang China. Quat Sci Rev 2016;146:134-46.
- [16] Xu H, Zhou K, Lan J, et al. Arid Central Asia saw mid-Holocene drought. Geology 2019;47:255–8.
- [17] Rao Z, Wu D, Shi F, et al. Reconciling the 'westerlies' and 'monsoon' models: a new hypothesis for the Holocene moisture evolution of the Xinjiang region NW China. Earth-Sci Rev 2019;191:263–72.
- [18] Dong G. Understanding past human-environment interaction from an interdisciplinary perspective. Sci Bull 2018;63:1023–4.
- [19] Aizen EM, Aizen VB, Melack JM, et al. Precipitation and atmospheric circulation patterns at mid-latitudes of Asia. Int J Climatol 2001;21:535–56.
- [20] Draxler RR, Rolph GD. HYSPLIT (Hybrid Single Particle Lagrangian Integrated Trajectory) model access via NOAA ARL READY website (http://ready.Arl.Noaa. Gov/hysplit.Php); 2013.
- [21] Edwards RL, Chen JH, Wasserburg GJ. ²³⁸U–²³⁴U-²³⁰Th-²³²Th systematic and the precise measurement of time over the past 500,000 years. Earth Planet Sci Lett 1987:81:175–92.
- [22] Shen CC, Lawrence Edwards R, Cheng H, et al. Uranium and thorium isotopic and concentration measurements by magnetic sector inductively coupled plasma mass spectrometry. Chem Geol 2002;185:165–78.
- [23] Cheng H, Lawrence Edwards R, Shen CC, et al. Improvements in ²³⁰Th dating, ²³⁰Th and ²³⁴U half-life values, and U-Th isotopic measurements by multi-collector inductively coupled plasma mass spectrometry. Earth Planet Sci Lett 2013;371:82–91.
- [24] Breitenbach S, Rehfeld K, Goswami B, et al. Constructing proxy records from age models (COPRA). Clim Past 2012;8:1765–79.
- [25] Li D, Tan L, Guo F, et al. Application of Avaatech X-ray fluorescence corescanning in Sr/Ca analysis of speleothems. Sci China Earth Sci 2019;62:964.
- [26] Baker A, Ito E, Smart PL, et al. Elevated and variable values of ¹³C in speleothems in a British cave system. Chem Geol 1997;136:263–70.
- [27] Genty D, Blamart D, Ouahdi R, et al. Precise dating of Dansgaard-Oeschger climate oscillations in western Europe from stalagmite data. Nature 2003;421:833-7.

[28] Mcdermott F. Palaeo-climate reconstruction from stable isotope variations in speleothems: a review. Quat Sci Rev 2004;23:901–18.

- [29] Cheng H, Spötl C, Breitenbach SF, et al. Climate variations of Central Asia on orbital to millennial timescales. Sci Rep 2016;5:36975.
- [30] Wolff C, Plessen B, Dudashvilli AS, et al. Precipitation evolution of Central Asia during the last 5000 years. Holocene 2017;27:142–54.
- [31] Fairchild IJ, Treble PC. Trace elements in speleothems as recorders of environmental change. Quat Sci Rev 2009;28:449–68.
- [32] Treble P, Shelley JMG, Chappell J. High resolution sub-annual records of trace elements in a modern 1911–1992 speleothem from southwest Australia. Earth Planet Sci Lett 2003;216:141–53.
- [33] Hendy CH. The isotopic geochemistry of speleothems—I. The calculation of the effects of different modes of formation on the isotopic composition of speleothems and their applicability as palaeoclimatic indicators. Geochim Cosmochim Acta 1971;35:801–24.
- [34] Cheng H, Zhang PZ, Spötl C, et al. The climatic cyclicity in semiarid-arid central Asia over the past 500,000 years. Geophys Res Lett 2012;39:L01705.
- [35] Carolin SA, Walker RT, Day CC, et al. Precise timing of abrupt increase in dust activity in the Middle East coincident with 4.2 ka social change. Proc Natl Acad Sci USA 2019;116:67–72.
- [36] Lauterbach S, Witt R, Plessen B, et al. Climatic imprint of the mid-latitude Westerlies in the Central Tian Shan of Kyrgyzstan and teleconnections to North Atlantic climate variability during the last 6000 years. Holocene 2014;24:970–84.
- [37] Endo K, Sugai T, Haragucili T, et al. Lake level change and environmental evolution during the last 8000 years mainly based on Balkhash Lake cores in Central Eurasia. In: Proceedings of the Proceedings of the International Workshop on Toward a Sustainable Society in Central Asia: an Historical Perspective on the Future. 2012. p. 35–48.
- [38] Ricketts RD, Johnson TC, Brown ET, et al. The Holocene paleolimnology of Lake Issyk-Kul, Kyrgyzstan: trace element and stable isotope composition of ostracodes. Palaeogeogr Palaeoclimatol Palaeoecol 2001;176:207–27.
- [39] Ran M, Feng Z. Variation in carbon isotopic composition over the past ca. 46,000 yr in the loess–paleosol sequence in central Kazakhstan and paleoclimatic significance. Org Geochem 2014;73:47–55.
- [40] Rea DK, Leinen M. Asian aridity and the zonal westerlies: late Pleistocene and Holocene record of eolian deposition in the Northwest Pacific Ocean. Palaeogeogr Palaeoclimatol Palaeoecol 1988;66:1–8.
- [41] Liu S, Deng C, Xiao J, et al. Insolation driven biomagnetic response to the Holocene warm period in semi-arid East Asia. Sci Rep 2015;5:8001.
- [42] Cai Y, Chiang JCH, Breitenbach SFM, et al. Holocene moisture changes in western China, Central Asia, inferred from stalagmites. Quat Sci Rev 2017;158:15–28.
- [43] Zhang X, Jin L, Chen J, et al. Detecting the relationship between moisture changes in arid central Asia and East Asia during the Holocene by model-proxy comparison. Quat Sci Rev 2017;176:36–50.
- [44] Hong B, Gasse F, Uchida M, et al. Increasing summer rainfall in arid eastern-central Asia over the past 8500 years. Sci Rep 2014;4:5279.
- [45] Roberts N, Eastwood WJ, Kuzucuoğlu C, et al. Climatic, vegetation and cultural change in the eastern Mediterranean during the mid-Holocene environmental transition. Holocene 2011;21:147–62.
- [46] Cheng H, Sinha A, Verheyden S, et al. The climate variability in northern Levant over the past 20,000 years. Geophys Res Lett 2016;42:8641–50.
- [47] Goslin J, Fruergaard M, Sander L, et al. Holocene centennial to millennial shifts in North-Atlantic storminess and ocean dynamics. Sci Rep 2018;8:12778.
- [48] Zanchetta G, Bar-Matthews M, Drysdale RN, et al. Coeval dry events in the central and eastern Mediterranean basin at 5.2 and 5.6 ka recorded in Corchia (Italy) and Soreq caves (Israel) speleothems. Glob Planet Change 2014;122:130–9.
- [49] Roland TP, Daley TJ, Caseldine CJ, et al. The 5.2 ka climate event: evidence from stable isotope and multi-proxy palaeoecological peatland records in Ireland. Quat Sci Rev 2015;124:209–23.
- [50] Bond G, Kromer B, Beer J, et al. Persistent solar influence on North Atlantic climate during the Holocene. Science 2001;294:2130–6.
- [51] Li K, Liu X, Hu Y, et al. Long-term increasing productivity of high-elevation grassland caused by elevated precipitation and temperature. Rangel Ecol Manag 2020;73:156-61.
- [52] Li S. The birth of prehistoric Silk Roads: ethnic migrations and interactions in Eurasian steppes and northwest China. In: Luo F, editor. Archaeology along the Silk Roads. Beijing: Science Press; 2018. p. 76–81 (in Chinese).
- [53] Sinor D. The Cambridge history of early inner Asia. Cambridge: Cambridge University Press; 1990.
- [54] Spengler RN. Niche dwelling vs. Niche construction: landscape modification in the Bronze and Iron ages of central Asia. Hum Ecol 2014;42:813–21.
- [55] Miller NF. Agricultural development in western Central Asia in the Chalcolithic and Bronze Ages. Veg Hist Archaeobot 1999;8:13–9.
- [56] Kutzbach JE, Chen G, Cheng H, et al. Potential role of winter rainfall in explaining increased moisture in the Mediterranean and Middle East during periods of maximum orbitally-forced insolation seasonality. Clim Dyn 2014;42:1079–95.

- [57] Monserud R, Denissenko O, Tchebakova N. Comparison of Siberian paleovegetation to current and future vegetation under climate change. Clim Res 1993;3:143-59.
- [58] Baker JL, Lachniet MS, Chervyatsova O, et al. Holocene warming in western continental Eurasia driven by glacial retreat and greenhouse forcing. Nat Geosci 2017;10:430-5.
- [59] Baumer C. The history of Central Asia. London: I.B.Tauris Publishers; 2012.
 [60] Narasimhan VM, Patterson N, Moorjani P, et al. The genomic formation of South and Central Asia. bioRxiv 2018;292581.
- [61] Frachetti MD, Smith CE, Traub CM, et al. Nomadic ecology shaped the highland geography of Asia's Silk Roads. Nature 2017;543:193–8.



Liangcheng Tan received his Ph.D. degree in Quaternary Geology at Institute of Earth Environment, Chinese Academy of Sciences (IEECAS) in 2009. Since then, he has worked in IEECAS as an assistant professor, an associate professor, and a full professor. His research interest includes high-resolution climate proxies in speleothems, Holocene climate change, impacts and human adaption, Anthropocene environment change.